Author(s): Morishige, Ashley & Laine, Hannu & Schön, Jonas & Hofstetter, Jasmin & Haarahiltunen, Antti & Schubert, Martin & Savin, Hele & Buonassisi, Tonio

Title: Analysis of Different Models of Iron Precipitation in Multicrystalline Silicon

Year: 2014

Version: Post print

Please cite the original version:

Morishige, Ashley & Laine, Hannu & Schön, Jonas & Hofstetter, Jasmin & Haarahiltunen, Antti & Schubert, Martin & Savin, Hele & Buonassisi, Tonio. 2014. Analysis of Different Models of Iron Precipitation in Multicrystalline Silicon. The 40th IEEE Photovoltaic Specialists Conference, Denver, Colorado, USA, June 8-13, 2014. 3. DOI: 10.1109/pvsc.2014.6925566.

Analysis of Different Models of Iron Precipitation in Multicrystalline Silicon

Ashley E. Morishige[1], Hannu S. Laine[2], Jonas Schön[3], Jasmin Hofstetter[1], Antti Haarahiltunen[2], Martin C. Schubert[3], Hele Savin[2], Tonio Buonassisi[1]

[1]Massachusetts Institute of Technology, Cambridge, MA, 02139, USA
[2]Aalto University, Department of Micro and Nanosciences, Tietotie 3, 02150 Espoo, Finland
[3]Fraunhofer Institute for Solar Energy Systems (ISE), 79100 Freiburg, Germany

***Abstract* — Simulation of solar cell processing enables inexpensive and rapid process optimization. Over the last twenty years, several models describing the distribution and behavior of iron point defects and iron-silicide precipitates have been developed and incorporated into process simulations. The goal of this work is to elucidate what physics are needed to accurately describe industry-relevant as-grown impurity and defect distributions and processing conditions by simulating different material-processing combinations with each model. This rigorous comparison helps scientists and engineers choose the appropriate level of model complexity, and consequently simulation run time, based on material characteristics and processing conditions.**

***Index Terms* — iron, gettering, modeling, phosphorus, photovoltaics, precipitates, silicon, simulation, TCAD**

I. Introduction

Metal impurities in *p*-type crystalline silicon degrade minority carrier lifetime and solar cell efficiency in even trace concentrations [1]. Iron, especially in interstitial form (Fe_i), is detrimental because it is abundant in industrial environments and can limit electron lifetime. In an as-grown wafer, almost all of the iron is in the form of iron-silicide precipitates [2], which act as sources and sinks of Fe_i, especially during high-temperature processing steps. The detrimental effect of iron contamination can be mitigated by gettering, or engineering the distribution of interstitial and precipitated iron [3, 4].

Simulation can enable inexpensive and rapid optimization of gettering that is tailored to the characteristics of the input material [5]. Thus, several models of the nucleation, growth, and dissolution of iron-silicide precipitates have been developed [6-9]. The goal of this work is to match different physical assumptions in simulations to different conditions, including as-grown impurity distribution and annealing or phosphorus diffusion gettering (PDG) parameters.

The models analyzed in this contribution are summarized in Fig. 1. Two different aspects of solar cell fabrication are evaluated: ingot crystallization, involving slow cooling from high temperatures, and annealing, sometimes with phosphorus diffusion. In these models, the crystallization of a typical cast multicrystalline silicon (mc-Si) ingot is modeled at one point (0D) or in two dimensions (2D). Dislocations are sites where iron can precipitate. The point model assumes homogeneously distributed dislocations, does not explicitly account for diffusion of Fe_i between dislocations, and leads to 1D wafer-level process simulation. 2D models allow for heterogeneous spacing of structural defects. For the 2D simulations, we varied the structural defects to describe different types of Si material. The presence of dislocations (DL) but no grain boundaries can represent materials like mono-like and epitaxial silicon [9]. On the other hand, grain boundaries, defined as dense lines of dislocations, and dislocations (DL+GB) are present in conventional mc-Si.

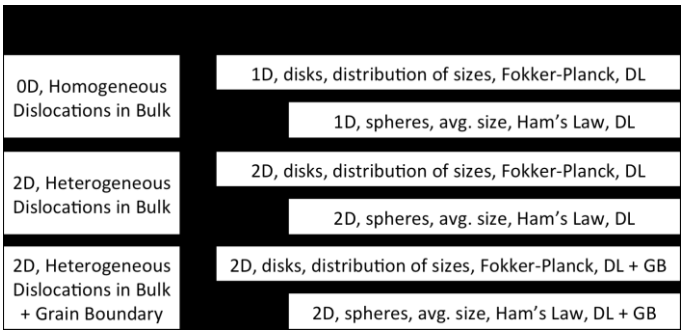

Fig. 1. Summary of simulation scenarios applied in this study.

The simpler iron precipitation model considered here describes precipitates as spheres with a single average radius that grows and dissolves according to Ham's law [10]. The more complex iron precipitation model considered describes precipitates as flat disks with a distribution of sizes that evolves according to the Fokker-Planck equations [11-13]. After the crystallization step, the average models are generated from the distributed models' average precipitate density and size. The six different wafer-level processing models are shown in the right column of Fig. 1. Phosphorus diffusion is simulated using the model suggested by Bentzen, *et al*. [14], and the iron segregation coefficient as a function of phosphorus doping is taken from Haarahiltunen, *et al.* [15].

Using each of these models, we simulate the Fe_i concentration after various processing conditions for several initial total iron concentrations. This side-by-side comparison elucidates the effects of the different assumptions between the models, enabling the matching of material and process complexity to the appropriate modeling assumptions.

II. Results

The crystallization of the mc-Si ingot is approximated as a linear cool from 1100°C to 200°C at a rate of 4 °C/min [12]. The Fe_i concentration as the solidification proceeds is shown in Fig. 2. Initially, all the iron is dissolved. As the solidification proceeds, the temperature and solubility drop and once a high enough supersaturation is achieved, iron precipitates nucleate and grow, reducing Fe_i. For an initial iron concentration of 10^{13} cm^{-3}, precipitation starts after ~125 min at ~600°C. For an initial concentration of 10^{14} cm^{-3}, the onset of precipitation is earlier at ~90 min and 740°C.

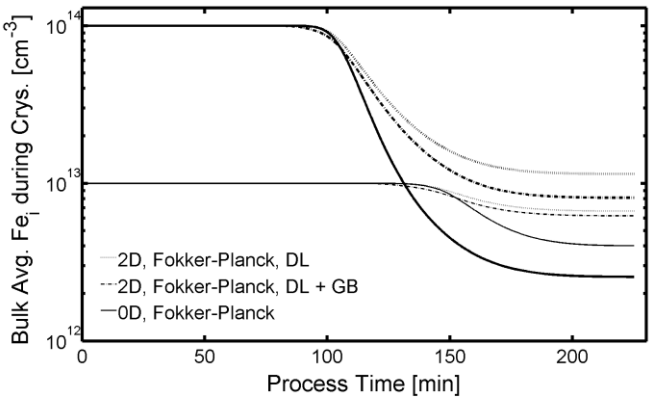

Fig. 2. Ingot crystallization. Interstitial iron concentration, Fe_i, as a function of ingot solidification time for initial Fe concentrations of 10^{14} cm^{-3} (thicker lines) and 10^{13} cm^{-3} (thinner lines).

The iron distribution at the end of ingot crystallization is the input to the phosphorus diffusion gettering step. The Fe_i concentration after a PDG consisting of a high-temperature plateau (850°C and 900°C) for 30 min followed by a ramp down at 4 °C/min to 700°C is plotted in Fig. 3 for three different initial total iron concentrations. A surface phosphorus concentration of 10^{21} cm^{-3} was assumed. Optimized for Fe defect reduction, not emitter formation, the 850°C plateau has a calculated sheet resistance of 39 Ω/□, and the 900°C resulted in a 17 Ω/□ emitter. Both PDG treatments significantly reduce the bulk average Fe_i for all initial iron concentrations. As the initial iron concentration increases, the model predictions do vary more, but the range is still small. For an initial iron concentration of 10^{13} and 10^{14} cm^{-3}, the bulk Fe_i concentration is reduced more by the 900°C than the 850°C PDG, and the resulting Fe_i is externally gettered to the phosphorus-rich layer. For the 10^{13} cm^{-3} case, precipitates are fully dissolved by both PDG temperatures. For the 10^{14} cm^{-3} case, after PDG at 850°C, small precipitates with radius up to 13 nm remain (Ham's Law DL case), but 900°C results in full dissolution. Higher temperature (~1050°C) is required to achieve the same effect for the 10^{15} cm^{-3} material, in which precipitates up to ~40 nm remain even after the 900°C PDG.

A low-temperature anneal (LTA) following PDG can decrease Fe_i and thereby increase electron lifetime if the time and temperature are chosen such that the solubility is low enough to prevent significant precipitate dissolution but the diffusivity is high enough to allow gettering [16]. For a typical initial iron concentration of 10^{14} cm^{-3} and after the 850°C PDG described above, we simulated the Fe_i concentration after 30 min LTA's at temperatures from 500 to 700°C (Fig. 4). A ramp rate of 4 °C/min from 700°C to the annealing temperature was assumed. The scenarios have similar predictions for LTA temperature greater than 600°C with the Ham's Law models predicting slightly higher Fe_i concentration but they increasingly diverge for lower temperatures, with the 1D models predicting a lower Fe_i concentration. The 1D models predict 525°C as the optimal LTA temperature while the 2D models indicate 550°C. The 2D DL only cases were very similar to the DL+GB only cases.

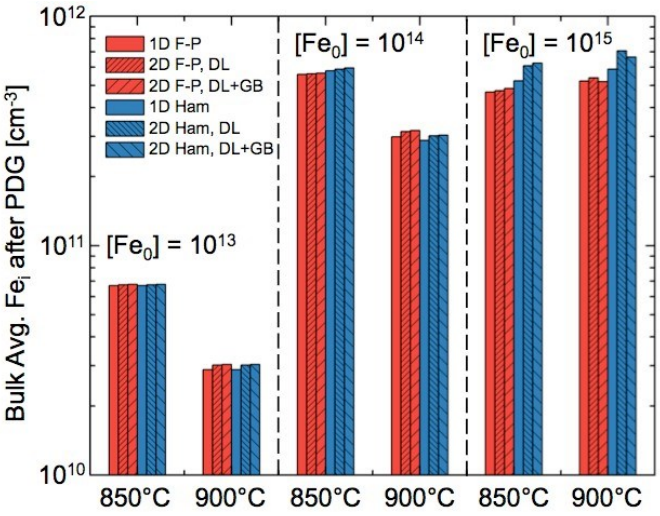

Fig. 3. PDG. Interstitial iron concentration, Fe_i, after PDG at 850°C and at 900°C followed by a 4 °C/min cool to 700°C as a function of initial total iron concentration, Fe_0, of 10^{13}, 10^{14}, and 10^{15} cm^{-3}. Fokker-Planck models are shown in red with Ham's Law in blue.

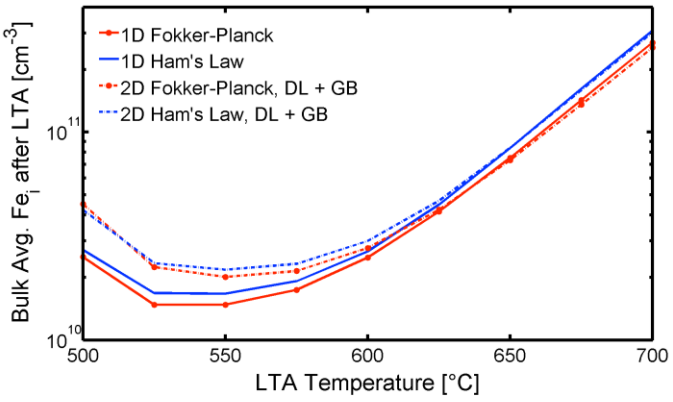

Fig. 4. Low temperature annealing after 850°C PDG for initial iron concentration of 10^{14} cm^{-3}. The models match well at and above 600°C, but they diverge for lower LTA temperatures.

III. Discussion

For the ingot solidification, the 2D DL only and 2D DL + GB cases predict similar Fe_i because the grain boundary has a small internal gettering effect relative to the dislocations in the bulk for the parameters assumed. The point model predicts the lowest Fe_i concentration because it models dislocations as homogeneously distributed and does not account for interstitials diffusing to precipitates. The results of the point model reveal a different trend compared to the 2D model, *i.e.* a lower Fe_i for the higher initial iron concentration.

During PDG, a dynamic steady state Fe_i concentration develops in which the increase of Fe_i due to precipitate dissolution is balanced by a decrease in Fe_i due to external gettering to the phosphorus-rich layer [10]. Once established, this dynamic balance removes Fe_i from the bulk at a rate that is fairly insensitive to differences in the precipitation models, *i.e.* dissolution rates are nearly the same in different models.

For the LTA's, above approximately 600°C, the solubility and diffusivity are high enough to establish the dynamic steady state described above and external gettering dominates. Below ~600°C, as the LTA temperature decreases, internal gettering of Fe_i to precipitates gets more important, and the differences between the models is more pronounced. Consistent with the crystallization results, the 1D Fokker-Planck model predicts the fastest precipitate growth and thus the lowest Fe_i, then the 1D Ham's law, then the 2D cases. Nonetheless, consistent with experimental findings in [16], all the scenarios agree that 525-550°C is the range of LTA temperatures that most effectively reduces the concentration of Fe_i.

IV. Significance of Work

Simulation of solar cell processing can facilitate the development of higher efficiency devices. However, the run time can vary by a factor of 20 or more, so using a model that is more complex than necessary can significantly slow the pace of optimization without a gain in accuracy. This comparison enables the selection of the appropriate level of model complexity based on material and processing parameters so that optimizations can be done efficiently but still accurately.

V. Summary

We compared several process simulation models to enable the matching of model assumptions to material and processing parameters. For the investigated phosphorus diffusion and low-temperature annealing conditions, the models predict similar average bulk interstitial iron concentration. A model that accounts for a distribution of precipitate sizes (Fokker-Planck) may be necessary when simulating high initial iron concentrations or gettering in areas with a high density of structural defects. 2D modeling is essential when analyzing inherently multi-dimensional phenomena such as the effect of dislocation density and crystal grain size on the iron distribution. Further simulations and analysis will be presented in a follow-up publication.

Acknowledgments

This material is based upon work supported by the National Science Foundation (NSF) and the Department of Energy (DOE) under NSF CA No. EEC-1041895. Authors from Aalto University acknowledge the financial support from Finnish Technology Agency and Academy of Finland. Authors from Fraunhofer ISE acknowledge the financial support by the German Federal Ministry for the Environment, Nature Conservation and Nuclear Safety within the research cluster "SolarWinS" (contract No. 0325270A-H). A. E. Morishige acknowledges the support of the Department of Defense through the NDSEG fellowship program. J.H. acknowledges support by the A. von Humboldt Foundation through a Feodor Lynen Postdoctoral Fellowship.

References

[1] A. A. Istratov, T. Buonassisi, R. J. McDonald, A. R. Smith, R. Schindler, J. A. Rand, J. Pl. Kalejs, and E. R. Weber, *J. Appl. Phys.*, vol. 94, pp. 6552-6559, 2003.

[2] D. Macdonald, A. Cuevas, A. Kinomura, Y. Nakano, and L. J. Geerligs, *J. Appl. Phys.*, vol. 97, 2005.

[3] B.L. Sopori, L. Jastrzebski, and T. Tan, *25th IEEE PVSC*, 1996, p. 625.

[4] A. A. Istratov, H. Hieslmair, and E. R. Weber, *Appl. Phys. A*, vol. 70, pp. 489-534, 2000.

[5] J. Hofstetter, J.-F. Lelièvre, D. P. Fenning, M. I. Bertoni, T. Buonassisi, and C. del Cañizo, *Solid State Phenomena*, vol. 178-179, pp. 158-165, 2011.

[6] M. Seibt, H. Hedemann, A.A. Istratov, F. Riedel, A. Sattler, and W. Schröter, *Phys. Stat. Sol. (a)*, vol. 171, pp. 301-10, 1999.

[7] S. Plekhanov, and T. Y. Tan, *Appl. Phys. Lett.* , vol. 76, 2000.

[8] C. Del Cañizo and A. Luque, *J. Electrochemical Society*, vol. 147, pp. 2685-92, 2000.

[9] R.B. Bergmann, *Appl. Phys. A*, vol. 69, pp. 187-194, 1999.

[10] J. Hofstetter, D. P. Fenning, M. I. Bertoni, J.F. Lelièvre, C. del Cañizo, and T. Buonassisi, *Prog. Photovolt. Res. Appl.*, vol. 19, pp. 487-497, 2011.

[11] S. Dunham, *Appl. Phys. Lett.*, vol. 63, pp. 464, 1993.

[12] A. Haarahiltunen, H. Savin, M. Yli-Koski, H. Talvitie, M. I. Asghar, and J. Sinkkonen, *Mater. Sci. Eng., B*, vol. 159-160, pp. 248-252, 2009.

[13] J. Schön, H. Habenicht, M. C. Schubert, and W. Warta, *J. Appl. Phys.*, vol. 109, 2011.

[14] A. Bentzen, A. Holt, J. S. Christensen, and B. G. Swensson, *J. Appl. Phys.*, vol. 99, 064502, 2006.

[15] A. Haarahiltunen, H. Savin, M. Yli-Koski, H. Talvitie, and J. Sinkkonen, *J. Appl. Phys.*, vol. 105, 023510, 2009.

[16] M. Rinio, A. Yodyunyong, S. Keipert-Colberg, Y. P. Botchak Mouafi, D. Borchert, and A Montesdeoca-Santana, *Prog. Photovolt. Res. Appl.*, vol. 19, pp. 165-169, 2011.